

Crystallographic Studies and Structural Systematics of the $C2/c$ Alkali Metal Metavanadates

H. N. NG, C. CALVO*, AND K. L. IDLER

Institute for Materials Research, McMaster University, Hamilton, Ontario, Canada. L8S 4M1

Received April 22, 1978; in revised form June 22, 1978

Four compounds in the system $(\text{Li, Na})\text{VO}_3$ were synthesized and their structures refined in the space group $C2/c$. Site population analysis showed that their compositions are $(\text{Na}_{0.5}\text{Li}_{0.5})\text{VO}_3$, $(\text{Na}_{0.62}\text{Li}_{0.38})\text{VO}_3$, $(\text{Na}_{0.71}\text{Li}_{0.29})\text{VO}_3$ and $(\text{Na}_{0.84}\text{Li}_{0.16})\text{VO}_3$. All have the structure of LiVO_3 and $\alpha\text{-NaVO}_3$ which are related to the $C2/c$ silicate pyroxenes. Structural data of eight compounds in the system $(\text{K, Na, Li})\text{VO}_3$ were compiled, and correlations were established by multiple regression analyses between the effective ionic radii r_{M1} and r_{M2} of the alkali metal ions and various structural parameters. The size of the $M2$ site and the relative displacement of the $(\text{VO}_3)_\infty$ chains are found to depend primarily on r_{M2} only. The size of the $M1$ site and the amount of chain rotation are affected by both r_{M1} and r_{M2} . Changes in lattice parameters are related to the chain movements. The anomalous chain configuration of LiVO_3 is also discussed.

Introduction

The structures of the alkali metal metavanadates are characterized by $(\text{VO}_3)_\infty$ chains formed by vertex sharing VO_4 tetrahedra. They are thus closely related to the silicate pyroxenes, and like the latter, also fall into two main groups. The metavanadates with small alkali metal cations LiVO_3 (1), $\alpha\text{-NaVO}_3$ (2-4) and $\text{NaK}(\text{VO}_3)_2$ (5) are monoclinic with the space group $C2/c$, and the larger ones KVO_3 , RbVO_3 and CsVO_3 (6) are orthorhombic with the space group $Pbcm$. In the $C2/c$ pyroxene-like metavanadates, adjacent VO_4 tetrahedra are related by the c -glide plane to form a chain parallel to the c -axis. Other chains are generated by the C -centering and twofold symmetry operations. The two types of metal cation

sites lie between the chains. Following the nomenclature of Burnham *et al.* (7) for the silicates, the smaller site is usually labelled as $M1$ and the larger site $M2$, and the bridging oxygen atom in the tetrahedral chain is labelled as $\text{O}3$. The configuration of the chain may be S -rotated as in LiVO_3 or O -rotated as in the rest, as defined by Thompson (8) and Papike *et al.* (9) for the silicate pyroxenes. All the known orthorhombic alkali metal metavanadates have extended or E chains (6).

In a previous account of our study (5) on cation substitution in the system $(\text{Na, K})(\text{V, P})\text{O}_3$, hereafter referred to as paper I, it was concluded that the size of the cation in the $M2$ site could be correlated with the rotation and displacement of the rigid $(\text{VO}_3)_\infty$ chains. The chain rotation may be measured by the parameter ϕ , or better by $\delta-\epsilon$ and the chain displacement may be

* Deceased.

measured by the parameter Δ as defined in (5). There have appeared in the literature many discussions on the crystal-chemical systematics of the $C2/c$ silicate pyroxenes (see e.g., references cited in (5) and (6)), and a recent account was reported by Ribbe and Prunier (10) who based their analysis on 13 "end-members" of the ordered $C2/c$ silicate pyroxenes. In order to make a comparative study of the structural systematics between the silicate and metavanadate pyroxenes, structural information on the latter with respect to varying the size of the $M1$ cations was needed. In the present study a series of compounds in the system $(\text{Li}, \text{Na})\text{VO}_3$ with different Na/Li ratios were synthesized. The results of their structural refinements were analysed by the technique of multiple linear regression analysis in a comparative study with the silicates.

Experiments

Crystals of $(\text{Na}_x\text{Li}_{1-x})\text{VO}_3$ were grown from mixtures of Na_2CO_3 , Li_2CO_3 and V_2O_5 in the appropriate molar ratios. The Na_2CO_3 used was preheated at 330°C for 6 hr before weighing. Four different mixtures with Na/Li ratio of 1:1, 1.5:1, 2.5:1 and 5:1 were melted in Pt crucibles at 900°C and cooled at the rate of 3°C/hr to 200°C , then quenched to room temperature. All the crystals are pale greyish and cylindrical in shape. Good quality single crystals were ground to spherical shapes ($r \approx 0.15$ mm) and examined by taking precession photographs before intensity measurements were made on a Syntex $P\bar{1}$ automatic diffractometer. Graphite-monochromatized $\text{MoK}\alpha$ radiation ($\lambda = 0.71069 \text{ \AA}$) was used in the $\theta/2\theta$ scan mode at variable scan rates. In all cases the conditions for systematic absences were $h+k \neq 2n$ for hkl and $l \neq 2n$ for $h0l$. The 2θ values of 15 reflections ($20^\circ < 2\theta < 45^\circ$) were carefully measured on the diffractometer and were used to obtain accurate lattice parameters (Table V) by least-squares refinements. The intensity data

were corrected for Lorentz and polarization effects.

Attempts were also made to prepare crystals with $\text{Na}/\text{Li} < 1$. However phase separation was observed in every crystal examined. The precession photographs showed two lattices with their b^* axes and c^* axes oriented in the same direction but with slightly different cell dimensions. The cell dimensions suggest that one of the phases is very close to LiVO_3 and the other a $(\text{Na}_x\text{Li}_{1-x})\text{VO}_3$ with $x > 0.5$. No intensities were measured on any of these crystals.

Structure Refinements

The structures were refined by least-squares methods as described in paper I. The refined population parameters for the cation sites indicate that the compositions of the four crystals are $(\text{Na}_{0.5}\text{Li}_{0.5})\text{VO}_3$, $(\text{Na}_{0.62}\text{Li}_{0.38})\text{VO}_3$, $(\text{Na}_{0.71}\text{Li}_{0.29})\text{VO}_3$ and $(\text{Na}_{0.84}\text{Li}_{0.16})\text{VO}_3$. These correspond to Na/Li ratios of 1:1, 1.6:1, 2.45:1 and 5.15:1 and will be referred to hereafter as compound I, II, III and IV respectively. Table I summarizes details of the refinements. The coefficients a , b , c and d used in the weighting function

$$w = [a + b|F_o| + c|F_o|^2 + d(\sigma/F_o)^2]^{-1}$$

are 0.8, -0.01 , 0.0002 and 850 respectively for all crystals. Positional parameters are listed in Table II and anisotropic thermal parameters in Table III. The important bond lengths and angles are shown in Table IV. Tables of structural amplitudes have been deposited.¹

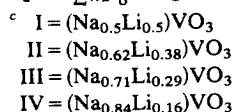
¹ See NAPS document No. 00000 for 18 pages of supplementary material. Order from NAPS c/o Microfiche Publications, P.O. Box 3513, Grand Central Station, New York, New York, 10017. Remit in advance for each NAPS accession number. Institutions and Organizations may use purchase orders when ordering, however, there is a billing charge of \$5.00 for this service. Make checks payable to Microfiche Publications. Photocopies are \$5.00. Microfiche are \$3.00 each. Outside the United States and Canada, postage is \$3.00 for a photocopy and \$1.00 for a fiche.

TABLE I
 COMPOSITION AND REFINEMENT DATA

	I ^c	II	III	IV
Site occupancy ^a	—	0.444(3)	0.578(4)	0.764(4)
% Na in <i>M1</i>	0	23.4	42.9	67.5
Total unique reflections	945	1143	970	1197
Number of reflections with $I > 3\sigma$	786	718	682	749
<i>R</i>	0.030	0.039	0.037	0.037
<i>R</i> _w ^b	0.031	0.027	0.031	0.034

^a Refers to the refined occupancy factor of site *M1* using a Na scattering curve. A Li scattering curve was used for site *M1* of I.

$$b \left[\frac{\sum w(|F_o| - |F_c|)^2}{\sum wF_o^2} \right]^{1/2}$$


 TABLE II
 POSITIONAL PARAMETERS (e.s.d.'s IN PARENTHESES)

Atom		<i>x</i>	<i>y</i>	<i>z</i>
<i>M1</i>	I	0	0.9142(8)	1/4
	II	0	0.9135(4)	1/4
	III	0	0.9143(4)	1/4
	IV	0	0.9135(3)	1/4
<i>M2</i>	I	0	0.2934(2)	1/4
	II	0	0.2943(2)	1/4
	III	0	0.2948(2)	1/4
	IV	0	0.2943(2)	1/4
V	I	0.28888(4)	0.09216(4)	0.24499(7)
	II	0.28988(4)	0.09160(5)	0.24920(7)
	III	0.29049(5)	0.09126(5)	0.25234(8)
	IV	0.29117(6)	0.09058(6)	0.25602(9)
O1	I	0.1171(2)	0.0949(2)	0.1479(3)
	II	0.1202(2)	0.0962(2)	0.1530(3)
	III	0.1226(2)	0.0978(3)	0.1563(3)
	IV	0.1250(2)	0.0991(3)	0.1594(4)
O2	I	0.3503(2)	0.2609(2)	0.2959(4)
	II	0.3506(2)	0.2573(2)	0.3028(3)
	III	0.3525(3)	0.2558(3)	0.3093(4)
	IV	0.3537(3)	0.2524(3)	0.3140(4)
O3	I	0.3561(2)	0.0011(2)	0.0318(3)
	II	0.3551(2)	0.0040(2)	0.0326(3)
	III	0.3549(2)	0.0054(2)	0.0337(3)
	IV	0.3533(2)	0.0061(3)	0.0352(4)

All the four compounds studied have been found to crystallize with the α -NaVO₃ structure (2–4). They are, therefore, related to the silicate clinopyroxenes. Compound I is an ordered structure with Li occupying the *M1* sites only and the Na in the *M2* sites only. It may therefore be considered as the fourth “end-member” in the series of known metavanadate clinopyroxenes. It has an almost extended chain (8, 9) with an 03-03(4)-03' angle of 179.2°, but still has a monoclinic and not an orthorhombic structure. In all four compounds the chains are *O*-rotated and both *M1* and *M2* are sixfold coordinated.

Regression Analysis

The technique of multiple linear regression analysis has often been used to provide a relationship between a dependent variable and two or more independent variables. The two independent variables that are of interest to us in this case are the size of the *M1* and *M2* cations, r_{M1} and r_{M2} . Various structural parameters may be chosen as the dependent variable *y*; but the obvious ones

TABLE III
 ANISOTROPIC THERMAL PARAMETERS (e.s.d.'s IN PARENTHESES) $\times 10^4$

Atom		U_{11}	U_{22}	U_{33}	U_{12}	U_{13}	U_{23}
M1	I	182(27)	208(30)	259(30)	0	78(23)	0
	II	192(16)	236(18)	192(15)	0	60(11)	0
	III	188(15)	211(16)	188(14)	0	60(10)	0
	IV	201(12)	204(12)	189(11)	0	38(8)	0
M2	I	236(8)	158(7)	290(9)	0	20(6)	0
	II	248(8)	199(8)	257(8)	0	-5(6)	0
	III	279(10)	173(9)	240(9)	0	-14(7)	0
	IV	298(11)	206(10)	242(9)	0	-44(8)	0
V	I	99(1)	105(1)	99(1)	-2(2)	41(1)	-5(2)
	II	125(1)	152(1)	87(1)	3(2)	37(1)	-6(2)
	III	140(2)	143(2)	81(2)	6(3)	33(1)	-3(2)
	IV	139(2)	156(2)	83(1)	3(2)	21(1)	-4(2)
O1	I	129(7)	189(8)	176(7)	19(7)	46(6)	11(8)
	II	154(7)	301(9)	185(7)	63(9)	43(6)	7(9)
	III	168(9)	286(11)	189(8)	57(11)	40(7)	17(10)
	IV	169(10)	269(12)	173(9)	46(11)	29(7)	12(10)
O2	I	261(10)	140(8)	260(10)	-52(8)	82(8)	-14(7)
	II	330(11)	201(9)	248(9)	-33(8)	84(8)	-21(7)
	III	392(14)	179(11)	224(10)	-54(10)	74(10)	-23(9)
	IV	370(15)	196(12)	257(12)	-67(11)	35(11)	-10(9)
O3	I	145(7)	219(9)	137(8)	14(7)	49(6)	-46(7)
	II	152(7)	282(9)	125(7)	13(7)	44(6)	-47(7)
	III	174(9)	269(11)	118(8)	-1(9)	48(7)	-44(8)
	IV	180(10)	280(12)	148(9)	12(9)	21(8)	-70(8)

that are expected to show a correlation with r_{M1} and r_{M2} are the cell parameters, the mean $M1-O$ distance $\langle M1-O \rangle$, the mean $M2-O$ distance $\langle M2-O \rangle$, the mean $V-O$ distance $\langle V-O \rangle$, the mean V to bridging oxygen distance $\langle V-O3 \rangle$, and the chain rotation and displacement parameters. The correlation in each case is established by computing the regression coefficients β 's for the regression equation

$$y = \beta_0 + \beta_1 r_{M1} + \beta_2 r_{M2}$$

by least-squares methods which minimize $\sum (y - y_{\text{obs}})^2$. The data for the analysis were taken from eight compounds in the system $(Li, Na, K)VO_3$ consisting of four "end-members" and four "solid solutions". They are tabulated in Table V. The effective ionic radii of Shannon and Prewitt (11) were used as a measure of r_{M1} and r_{M2} . In the cases

where the cation site may be occupied by two different alkali metal atoms, the effective ionic radius was assumed to be a linear function of the chemical composition of that site. The computer program BMPD2R in the Biomedical Computer Programs by Dixon (12) was used. Table VI lists the regression coefficients β 's, the maximum residual (i.e., $(y - y_{\text{obs}})_{\text{max}}$), the standard error of estimate S , the correlation index R^2 and the F ratio. In most cases the maximum residual was found in $LiVO_3$, the only compound in the whole series with an S -rotated chain. Subsequently the data for $LiVO_3$ was given only half of the weight, and in some cases zero weight.

(i) The VO_4 Tetrahedron

In paper I we pointed out that the size of the $M2$ polyhedron had no effect on the size

TABLE IV
BOND GEOMETRY (e.s.d.'s IN PARENTHESES)

Bond	Distance (Å)			
	I	II	III	IV
<i>M1</i> -O1(2) ^a	2.240(2)	2.285(2)	2.320(1)	2.344(2)
-O1	2.219(6)	2.257(4)	2.283(4)	2.329(3)
-O2	2.142(4)	2.191(4)	2.219(4)	2.257(4)
⟨ <i>M1</i> -O⟩	2.200	2.244	2.274	2.310
<i>M2</i> -O1	2.340(2)	2.363(2)	2.377(3)	2.396(3)
-O2	2.638(2)	2.616(2)	2.593(2)	2.566(2)
-O3(5)	2.468(2)	2.510(2)	2.534(3)	2.569(3)
⟨ <i>M2</i> -O⟩	2.482	2.496	2.501	2.510
V-O1	1.653(2)	1.652(2)	1.649(2)	1.647(2)
-O2	1.642(2)	1.631(2)	1.639(3)	1.635(3)
-O3	1.806(2)	1.801(2)	1.804(2)	1.804(3)
-O3(4)	1.801(2)	1.802(2)	1.806(2)	1.800(2)
⟨V-O⟩	1.725	1.721	1.724	1.721

Bonds	Angles (deg.)			
	I	II	III	IV
O1(2)- <i>M1</i> -O1(4)	175.8(4)	175.5(2)	174.5(2)	174.3(2)
-O1	84.1(1)	85.9(1)	87.3(1)	88.4(1)
-O1(3)	99.0(2)	97.5(1)	96.7(1)	95.8(1)
-O2(5)	87.0(1)	87.1(1)	87.1(1)	87.2(1)
-O2(7)	90.2(2)	90.0(1)	89.3(1)	89.0(1)
O1- <i>M1</i> -O1(3)	84.9(3)	84.4(2)	84.4(2)	84.1(1)
-O2(5)	168.1(2)	169.6(1)	171.1(1)	172.1(1)
-O2(7)	88.7(1)	88.98(8)	89.3(1)	89.8(1)
O2(5)- <i>M1</i> -O2(7)	99.2(3)	98.6(2)	97.6(1)	96.6(1)
O1- <i>M2</i> -O1(3)	79.6(1)	79.8(1)	80.4(1)	81.2(1)
-O2(6)	86.48(7)	85.26(7)	84.47(7)	84.2(1)
-O2(8)	76.96(7)	78.79(7)	79.71(8)	81.0(1)
-O3(5)		137.35(6)	138.11(7)	139.15(8)
-O3(7)		115.91(6)	115.20(7)	114.19(8)
O2(6)- <i>M2</i> -O3(5)		134.98(8)	134.8(1)	133.8(1)
-O3(7)		64.49(6)	64.59(7)	64.41(8)
-O2(8)	158.5(1)	159.2(1)	159.3(1)	160.5(1)
O3(5)- <i>M2</i> -O3(7)		80.28(7)	80.03(8)	79.65(9)
O1-V-O2	110.2(1)	109.8(1)	109.7(1)	109.5(1)
-O3	111.6(1)	111.3(1)	111.1(1)	110.7(1)
-O3(4)	111.3(1)	111.4(1)	112.0(1)	111.8(1)
O2-V-O3	110.0(1)	110.1(1)	110.0(1)	109.9(1)
-O3(4)	105.2(1)	105.6(1)	105.2(1)	105.5(1)
O3-V-O3(4)	108.3(9)	108.6(1)	108.6(1)	109.1(1)
O3(4)-O3-O3(4) ^c	179.2(1)	177.1(1)	176.1(1)	175.6(1)

^a The position of an atom *A*(*n*) is derived from that of *A* shown in Table II by the *n*th symmetry operation as appears in the International Tables for X-ray Crystallography, Vol. I (1965) for the space group *C2/c*. For example, O1(2) is related to O1 by the symmetry operation $\bar{x}, \bar{y}, \bar{z}$.

TABLE V

EFFECTIVE IONIC RADII, LATTICE PARAMETERS, MEAN BOND LENGTHS AND CHAIN ROTATION AND DISPLACEMENT PARAMETERS FOR 8 ALKALI METAL METAVANADATES (e.s.d.'s ARE SHOWN IN PARENTHESES) FOR LATTICE PARAMETERS MEASURED IN THIS WORK

	LiVO ₃	I	II	III	IV	NaVO ₃	(Na _{0.88} K _{0.12}) VO ₃	(Na _{0.5} K _{0.5}) VO ₃
Ref.	3	this work	this work	this work	this work	5	1	1
$r_{M1}(\text{Å})$	0.740	0.740	0.806	0.860	0.929	1.020	1.020	1.020
$r_{M2}(\text{Å})$	0.740	1.020	1.020	1.020	1.020	1.020	1.110	1.380
$a(\text{Å})$	10.158	10.179(6)	10.280(5)	1.349(5)	10.446(4)	10.552	10.533	10.533
$b(\text{Å})$	8.417	9.061(4)	9.150(5)	9.218(5)	9.315(4)	9.468	9.580	9.997
$c(\text{Å})$	5.885	5.845(3)	5.850(3)	5.862(4)	5.869(2)	5.879	5.850	5.804
$\beta(\text{deg.})$	110.48	100.13(4)	108.75(4)	108.47(5)	108.57(3)	108.47	107.56	104.17
$c \sin \beta(\text{Å})$	5.513	5.522	5.539	5.552	5.564	5.576	5.577	5.628
$V(\text{Å}^3)$	471.4	509.33	521.06	530.41	541.46	557.1	562.8	592.6
$\langle M1-O \rangle(\text{Å})$	2.153	2.200	2.244	2.274	2.310	2.364	2.371	2.398
$\langle M2-O \rangle(\text{Å})$	2.284	2.483	2.496	2.501	2.510	2.513	2.572	2.780
$\langle V-O \rangle(\text{Å})$	1.725	1.725	1.721	1.724	1.721	1.723	1.717	1.722
$\langle V-3 \rangle(\text{Å})$	1.808	1.803	1.802	1.805	1.802	1.803	1.800	1.806
$\Delta(\text{Å})$	1.927	1.332	1.338	1.346	1.391	1.435	1.238	0.625
$\phi(\text{deg.})$	-19.2	0.78	2.87	3.86	4.42	5.45	8.04	12.00
$\delta-\epsilon(\text{deg.})$	-8.1	0.58	1.37	1.66	1.97	2.60	3.94	5.89

TABLE VI

RESULTS OF MULTIPLE REGRESSION ANALYSIS

Variable	Regression coefficients ^a						
	β_0	β_1	β_2	$(y - y_{\text{obs}})_{\text{max}}$	S	R^2	F
$\langle M1-O \rangle$	1.655	0.58(3)	0.12(2)	0.01	0.006	0.995	543
$\langle M2-O \rangle$	1.673	0.09(2)	0.73(1)	0.007	0.005	0.999	2079
a	9.231	1.29(5)	—	0.027	0.015	0.992	735
b	6.543	1.41(13)	1.44(11)	0.018	0.034	0.992	310
c	5.954	0.11(3)	-0.19(2)	0.011	0.006	0.951	49
β	120.18	-1.49(1.9)	-10.2(1.4)	1.05	0.48	0.941	96
	[122.13] ^b	[-1.7(8)]	[-11.7(6)]	[0.246]	[0.198]	[0.990]	[252]
$c \sin \beta$	5.288	0.17(4)	0.12(3)	0.016	0.009	0.953	51
V	274.10	165(12)	109(9)	6.54	3.00	0.994	432
	[285.94]	[164(5)]	[100(5)]	[2.23]	[1.40]	[0.998]	[1398]
Δ	3.275	0.41(5)	-2.22(4)	0.017	0.013	0.999	2129
ϕ	-46.6	18(16)	31(12)	10.0	4.2	0.78	9
	[-28.9]	[17(4)]	[17(3)]	[0.58]	[0.94]	[0.956]	[54]
$\delta-\epsilon$	-21.1	8(6)	15(5)	4.02	1.64	0.827	12
	[-14.1]	[7(1)]	[9(1)]	[0.20]	[0.37]	[0.971]	[83]

^a Standard errors for β_1 and β_2 in parentheses.

^b Values shown in square brackets were obtained by giving zero weight to the LiVO₃ data, which were otherwise given a weight of 0.5.

of the VO_4 tetrahedron. The remarkably constant dimension of the VO_4 tetrahedron is confirmed in this study simply by an inspection of Tables IV and V without resorting to regression analysis. Not only does the overall mean V-O distance $\langle \text{V-O} \rangle$ remain practically constant throughout the series, but so does the mean length of the two V-O_{bridging} bonds $\langle \text{V-O3} \rangle$. This is in direct contrast to the silicates where a positive correlation was found between $\langle \text{Si-O3} \rangle$ and r_{M1} and r_{M2} (10). It is not surprising then that the structural changes resulting from varying the size of the cations can be described by the rotational and translational movements of the chains in the alkali metal metavanadates.

(ii) The $\langle \text{M1-O} \rangle$ and $\langle \text{M2-O} \rangle$ Distances

Although both $\langle \text{M1-O} \rangle$ and $\langle \text{M2-O} \rangle$ are highly correlated with r_{M1} and r_{M2} respectively as expected, $\langle \text{M2-O} \rangle$ is almost independent of r_{M1} as indicated by the small regression coefficient of 0.09 (Table VI). However, $\langle \text{M1-O} \rangle$ shows a significant interdependence on r_{M2} . This may also be shown by a plot of $\langle \text{M2-O} \rangle$ versus r_{M2} , and $\langle \text{M1-O} \rangle$ versus r_{M1} (Fig. 1). The linear relationship between r_{M1} and $\langle \text{M1-O} \rangle$ holds only for the cases where r_{M2} remains constant due to the exclusive occupation of the $M2$ sites by Na. This is again in direct contrast to what was found in the silicates (10) where $\langle \text{M1-O} \rangle$ depends only on r_{M1} and $\langle \text{M2-O} \rangle$ depends on both r_{M1} and r_{M2} .

(iii) The Cell Dimensions

The most significant change in the cell dimensions across the series is in the b -axis (Table V), which is equally affected by both r_{M1} and r_{M2} with regression coefficients 1.41 and 1.44 respectively. However, when the observed values of b are plotted against those calculated from the regression equation (Fig. 2), the observed value for LiVO_3 falls far short of the predicted. It was noted in paper I that increasing the amount of chain rotation (both S and O) should be accom-

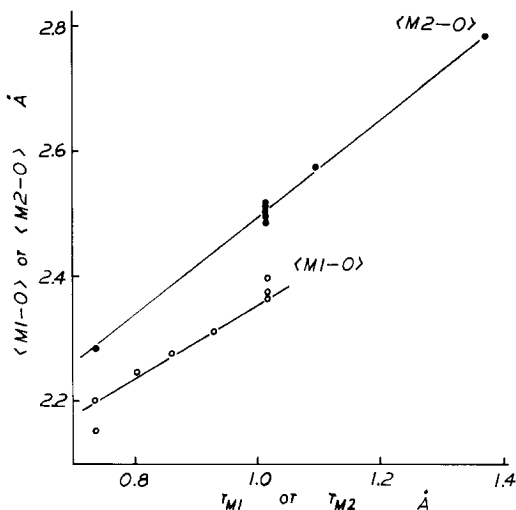


FIG. 1. Correlations between r_{M1} and $\langle \text{M1-O} \rangle$ and between r_{M2} and $\langle \text{M2-O} \rangle$ (regression lines are drawn with r_{M2} and r_{M1} held constant at 1.02 Å respectively).

panied by an increase in the b cell dimension. Figure 2 shows that there is definitely a positive correlation between b and the chain rotation parameter $\delta-\epsilon$. It appears that the change in b may be better interpreted as a

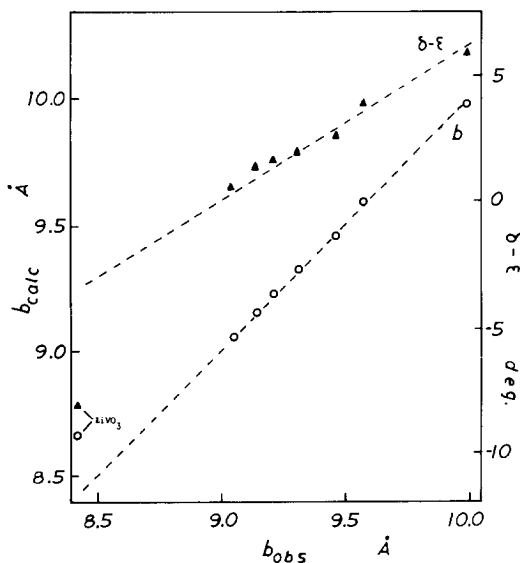


FIG. 2. Correlations between observed b and b calculated from the regression equation, and between b and $\delta-\epsilon$ (the straight lines are for better viewing only).

result of the change in chain rotation rather than an expansion of the "rift zone" envisaged by Ribbe and Prunier, with the exception of LiVO_3 where the much smaller than expected b -axis is caused by a genuine contraction of the "rift-zone" between the chains. This is also borne out by the unit cell volume V of LiVO_3 , which is about 6 \AA^3 smaller than the value predicted by the regression equation. The increased β angle cannot account for the small volume since the β angle of LiVO_3 is also smaller than expected, which should lead to a larger unit cell volume.

The a cell dimension was found to be linearly related to r_{M1} only, as in the case of silicate pyroxenes. The F ratio for r_{M2} was so small that consequently r_{M2} was removed from the step-wise regression analysis of a . Figure 3 shows the linear relationship between a and r_{M1} . Since the length of the a -axis is related to the separation between

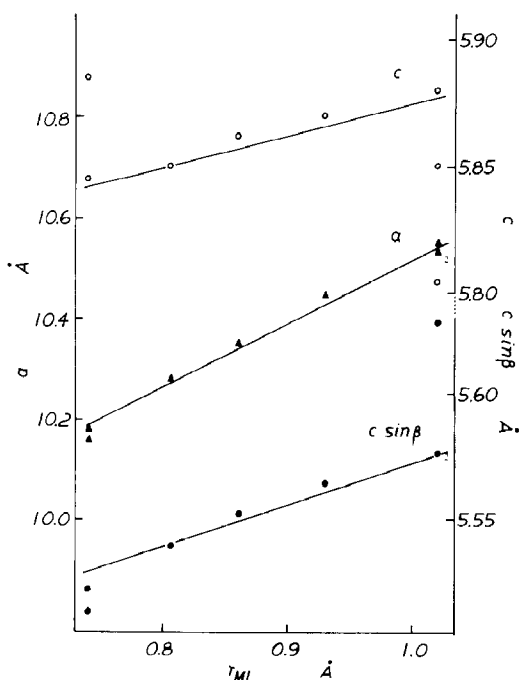


FIG. 3. Correlations between a , c , $c \sin \beta$ and r_{M1} (the regression lines are drawn with constant r_{M2} of 1.02 \AA).

the tetrahedral chain layers and is almost independent of r_{M2} , the results thus support the contention of Ribbe and Prunier (10) that the thickness of these layers were not affected by the size of the $M2$ polyhedra in the pyroxene structures.

In the silicates the quantity $c \sin \beta$ was found to be linearly related to r_{M1} but c and β separately were not (10). The regression coefficients for r_{M1} and r_{M2} are almost equal in magnitude both for the correlation of c and $c \sin \beta$ (Table VI) in the metavanadates. It may also be seen from Fig. 3 that the linear relationship between r_{M1} and c or $c \sin \beta$ only holds when r_{M2} is constant due to the exclusive occupation of $M2$ sites by Na. It must be borne in mind, however, that the variation of the c cell dimension across the series is very small compared with those in a and b . The maximum variations are 0.40 \AA , 1.58 \AA and 0.08 \AA for a , b and c respectively (Table V), and the F ratio for the analysis of c is also small compared with those for a and b (Table VI). Therefore not too much significance should be attached to the correlation of c or $c \sin \beta$ with the sizes of the alkali metal cations.

Although the β angle changes from the 110.48° in LiVO_3 to 104.17° in $\text{NaK}(\text{VO}_3)_2$, the effect depends primarily on r_{M2} only. The regression coefficient for r_{M2} has a magnitude about 10 times that for r_{M1} (Table VI). A similar observation is also noted in the analysis of the chain displacement parameter Δ .

(iv) The Chain Displacement Parameter

In paper I the parameter Δ was used as a measure of the tetrahedral chain displacement in the $[001]$ direction, and they were shown to be almost linearly related to $\langle M2-O \rangle$ and therefore to r_{M2} . The regression coefficients (Table VI) not only confirm this observation but also indicate that the correlation is heavily in favour of r_{M2} in both β and Δ . This points to a significant feature of the metavanadate pyroxenes, i.e., the tetra-

hedral chain displacement is a function of the size of $M2$ only. The effect of r_{M1} on the chain displacement is very small and perhaps opposite to that of r_{M2} as can be seen from the signs and magnitudes of their regression coefficients. Once again the observed values of β and Δ for LiVO_3 fall short of the prediction. The improvements obtained in the correlation by removing LiVO_3 are obvious as shown by the standard errors of estimate, the correlation index R^2 and the F ratios (Table VI).

Discussions and Conclusions

The following conclusions may be drawn from this study of the $C2/c$ metavanadate pyroxenes.

(i) Increasing the size of the $M1$ cation results in an increase in $\langle M1-O \rangle$. The structure responds by expansion in the a cell dimension, which corresponds to a widening of the space between the tetrahedral layers. It also leads to a small increase in Δ and a small decrease in β .

(ii) Increasing the size of the $M2$ cation leads to an increase in $\langle M2-O \rangle$. The characteristic response of the structure to accommodate this change is a decreased amount of tetrahedral chain displacement in the $[001]$ direction, and hence a smaller β angle. This chain displacement appears to be a necessary mechanism to bring two additional bridging oxygen atoms from the tetrahedral chains closer into the primary coordination sphere of the $M2$ polyhedron.

(iii) Starting from an almost extended chain in $(\text{Na}_{0.5}\text{Li}_{0.5})\text{VO}_3$, an increase in either r_{M1} or r_{M2} results in an increased amount of chain rotation in the O direction. This in turn brings about an increase in the b cell dimension, which is a measure of the separation between adjacent chains in the same layer, in an apparent effort to reduce the repulsion between adjacent chains.

(iv) The dimensions of the VO_4 tetrahedron, in particular the bridging V-O3

bond length, is much less susceptible than the SiO_4 tetrahedron to changes brought about by varying the size of the non-tetrahedral cations.

Clearly the structure of LiVO_3 with an S rotated chain is unique in this series of alkali metal metavanadates. A continuous transition from an O rotated chain to an S rotated chain does not seem to be possible as evidenced by the exolution of a Na-rich metavanadate from an Li-rich metavanadate. The incompatibility of these two structures may arise from the need to have the same tetrahedral chain rotated both in the O and S directions since an Li-rich metavanadate, if it existed, would be a "solid solution". From the opposite signs of the regression coefficients for r_{M1} and r_{M2} (Table VI) with respect to Δ , it may be reasoned that as the tetrahedral chain becomes almost extended, further increase in chain displacement will increase the size of $M1$. This can only be compensated for by a chain rotation in the S direction, accompanied by a general contraction of the structure in order to maintain both $\langle M1-O \rangle$ and $\langle M2-O \rangle$ small. This would reduce the amount of chain displacement which would have resulted were it the only response of the structure to the introduction of a small $M2$ cation. The same argument could be applied to the $C2/c$ silicate pyroxenes where an S rotated chain is observed only in structures with Li occupying the $M2$ site (9).

Acknowledgments

This work has been supported by the National Research Council of Canada through an operating grant. We would also like to thank Mr. J. D. Garrett for his assistance in crystal growth, and Dr. I. D. Brown for helpful discussions.

References

1. R. D. SHANNON AND C. CALVO, *Canad. J. Chem.* **51**, 265 (1973).

2. C. T. PREWITT, A. SCROUG, S. SUENO, AND M. CAMERON, *Geol. Soc. Amer. Ab. Prog.* **4**, 630 (1972).
6. F. MARUMO, M. ISOBE, AND S. IAWI, *Acta Crystallogr. B* **30**, 1628 (1974).
4. K. RAMANI, A. K. SHAIKH, B. S. REDDY, AND M. A. WISWAMITRA, *Ferroelectrics* **9**, 49 (1975).
5. K. L. IDLER, C. CALVO, AND H. N. NG, *J. Solid State Chem.* (to appear in the July issue 1978).
6. F. C. HAWTHORNE AND C. CALVO, *J. Solid State Chem.* **22**, 157 (1977).
7. C. W. BURNHAM, J. R. CLARK, J. J. PAPIKE, AND C. T. PREWITT, *Z. Kristallogr.* **125**, 109 (1967).
8. J. B. THOMPSON, *Amer. Mineral.* **55**, 292 (1970).
9. J. J. PAPIKE, C. T. PREWITT, S. SUENO, AND M. CAMERON, *Z. Kristallogr.* **138**, 254 (1973).
10. P. H. RIBBE AND A. R. PRUNIER, *Amer. Mineral.* **62**, 710 (1977).
11. R. D. SHANNON AND C. T. PREWITT, *Acta Crystallogr., B* **25**, 925 (1969).
12. W. J. DIXON, Ed., *BMDP Biomedical Computer Programs*, University of California Press, Berkeley, 1975.